ELSEVIER

Journal of Power Sources 79 (1999) 242–249

JOURNAL OF POWER SOURCES

Testing tubular solid oxide fuel cells in nonsteady-state conditions

V.V. Kharton *, E.N. Naumovich, V.N. Tikhonovich, I.A. Bashmakov, L.S. Boginsky, A.V. Kovalevsky

Institute of Physicochemical Problems, Belarus State University, 14 Leningradskaya Str., Minsk 220080, Belarus

Received 8 September 1998; received in revised form 26 January 1999; accepted 1 February 1999

Abstract

Fabrication of tubular-type solid oxide fuel cells (SOFCs) with yttria-stabilized zirconia electrolyte, cathodes and current collectors of lanthanum–strontium manganite (LSM) is described. Particular emphasis is given to the techniques of producing LSM tubes by the isostatic pressing method, preparing oxide electrodes via cellulose precursor decomposition, and activation of SOFC electrodes by applying dispersed catalysts onto their surface. Coating nickel-cermet anodes with dispersed ceria and depositing praseodymium oxide onto manganite cathode surface was found to result in improving SOFC performance. Testing single cells with externally switched pulse load demonstrated a possibility to optimize the SOFC operating mode at a given resistance of the closing circuit by variation of the pulse period-to-pulse duration ratio of the pulses which open the circuit. No effect of the pulse load frequency on SOFC performance was observed in the frequency range from 2 Hz to 50 kHz. The results of testing SOFCs in nonsteady-state conditions suggest applicability of the externally switched pulse load to match resistances of single cells in the SOFC stacks.

Keywords: SOFC; Pulse load; Surface modification; Lanthanum–strontium manganite; Cellulose precursor

1. Introduction

Solid oxide fuel cells (SOFCs) possess many attractive features such as low emission of pollutant, low noise and high energy conversion efficiency [1,2]. However, fabrication of single cells and selection of materials still comprise an important part in the development of SOFC [3]. The state-of-the-art materials of the SOFC are: yttria-stabilized zirconia (YSZ), lanthanum–strontium manganites (LSM), cermets of nickel and YSZ, lanthanum chromite doped with alkaline-earth and transition elements [4–6]. Performance is governed by the electronic resistivities of the electrode electrocatalysts and interconnectors, overpotentials associated with charge transfer at the electrode–electrolyte–gas phase boundaries as well as rates of gas transport at the electrodes [5,7]. The electrode resistance was reported to be reduced by increasing ionic conductivity of the electrode materials [5], incorporating catalysts into the electrolyte surface layer [8] and onto electrode surface [9,10], optimizing microstructure of electrodes and electrode/electrolyte interfaces [11].

A number of our previous works was devoted to developing SOFC electrode materials and methods to improve electrode performance [10,12–16]. Electrodes of perovskite-type $La_{0.6-x}Sr_{0.4}MnO_{3-\delta}$ ($x = 0$–0.1) solid solutions having considerable oxygen ion transport properties with prevailing electronic conductivity [10,12,17,18], were found to exhibit a high electrochemical activity in contact with YSZ electrolytes and thermal expansion coefficients (TECs) close to that of stabilized zirconia ceramics [10,12]. In order to avoid formation of blocking layers between LSM and YSZ, it was recommended to use sintering aids of bismuth cuprate, Bi_2CuO_4, and metallic silver which results in a decreasing temperature of electrode sintering and reducing electrode resistance [10,12]. An increase in electrochemical activity of the LSM electrodes can be achieved by applying catalytic layers of praseodymium oxide and lanthanum–strontium cobaltite onto their surface [12,16]. Technologies to produce ceramics for electrochemical applications by isostatic pressing were reported in Ref. [19].

The present work is aimed at developing methods to fabricate single fuel cells and testing the cells in different operating conditions. Particular attention was focused on testing the SOFC under nonsteady-state conditions with

* Corresponding author. Tel.: +7-17-2207681; Fax: +7-17-2264696; E-mail: kharton@fhp.bsu.unibel.by

0378-7753/99/$ - see front matter
PII: S0378-7753(99)00176-7

cycling external load. Our interest in the nonstationary operation is associated with the necessity to match the external load resistance to the internal resistance of each cell of an SOFC stack in order to provide maximum efficiency of the stack. Since the voltage of a single cell with connected load is not sufficiently high (0.4–0.8 V) and the current is significant (at least, 250 mA/cm^2), the only acceptable version of electrical connection of single SOFCs is a series connection to achieve a voltage above 10 V. Therewith, a decrease in performance of a single cell due to time degradation of SOFC components or thermal cycling [4,20] may result in a considerable decrease of the SOFC stack performance. Alternatively, one can consider a pulse circuit consisting of a useful load equivalent (resistor) and externally controlled switch connected in series to a single cell. Such a scheme is assumed to vary effective load resistance by varying pulse the period-to-pulse duration ratio of the interrupting pulses. In addition, such connection converts SOFC voltage to a pulse voltage, which can be easily transformed further into alternating voltage using well-known electrical circuits. Thus, one of the goals of our research was to estimate the applicability of externally switched pulse load for optimizing operation of the single tubular-type SOFCs.

2. Experimental

2.1. Cell design

Schematic drawings of the fuel cells tested in this work are presented in Figs. 1 and 2. The SOFCs were fabricated using gas-tight tubes of the $Zr_{0.90}Y_{0.10}O_{1.95}$ solid electrolyte, manufactured by the Ukrainian Research Institute of Refractories (Kharkov, Ukraine). The mean wall thickness of the YSZ tubes was 0.7 mm. The anode current collectors of the SOFCs were fabricated using springs and tubes (or rods) of a Ni–Cr alloy. The electrode surface area was varied from 6 to 20 cm^2.

For the cell shown in Fig. 1, the cathode current collectors were made from dense tubes of the $La_{0.7}Sr_{0.3}MnO_{3-\delta}$ solid solution (LSM7) and high-porosity ceramics of $La_{0.6}Sr_{0.4}MnO_{3-\delta}$ (LSM6). The choice of LSM7 for producing ceramic tubes was based on the results of preliminary tests which showed that the ceramics of this oxide exhibit a better thermal shock resistance in comparison with other lanthanum–strontium manganites. Therewith, electrical conductivity of LSM7 is lower as related to that of LSM6. Since cracking of the current-collector ceramic tube would result in destruction of the cell drawn in Fig. 1, the tubes were made of LSM7 in order to improve their stability under the thermal cycling conditions. LSM6 was used as the material of the high-porosity ceramics in order to reduce electrical resistance of the current collectors. For forming porous LSM6 ceramics, dense granules (about 1.0 mm in diameter) of the lanthanum–strontium manganite were filled up between the LSM and YSZ tubes and coated with a paste containing dispersed LSM6 powder, organic binder (colophony) and isopropanol. After assembling the cell, the metallic spring at the anode was coated with a paste consisting of a Ni–YSZ cermet powder, the binder and isopropyl alcohol. Then the cell was subjected to sintering at 1320–1370 K for 4 h. In the course of the sintering, hydrogen and air flows were passed at the anode and cathode, respectively. The aim of this procedure was to improve electrical contacts between cell components. The methods of preparing cermets, LSM powders and ceramics are described below. Hereafter, the cell shown in Fig. 1 is referred to as cell 1.

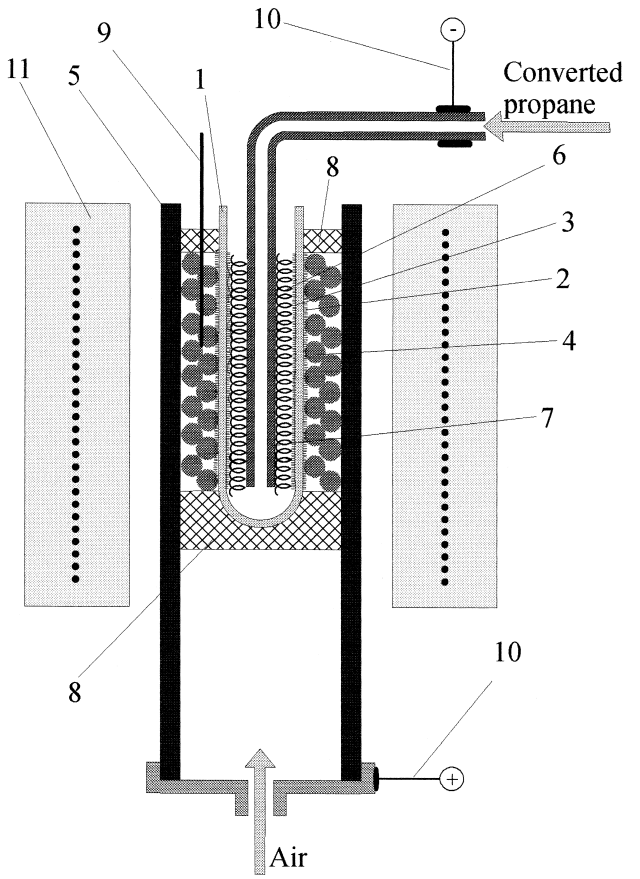

Fig. 1. Schematic drawing of SOFC with manganite current collectors: (1) YSZ tube, (2) LSM6 cathode, (3) Ni-cermet anode, (4) high-porosity LSM6 ceramics, (5) dense LSM7 tube, (6) metallic spring, (7) metallic tube, (8) porous ceramic insertions, (9) thermocouple, (10) copper current collectors, and (11) furnace.

The construction of the cell demonstrated in Fig. 2 (cell 2) is close to that of cell 1. The main difference is that the cathode current collectors of cell 2 were made of Pt wires (0.5 and 1 mm in diameter).

2.2. Fabrication of electrodes

In this work, SOFC cathodes were made of $La_{0.6}Sr_{0.4}MnO_{3-\delta}$ perovskite prepared by two methods: the

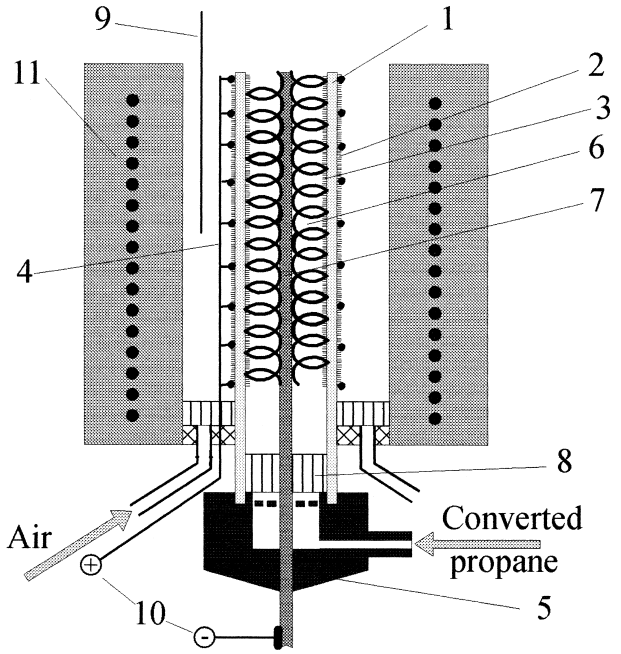

Fig. 2. Schematic drawing of SOFC with Pt current collectors: (1) YSZ tube, (2) LSM6 cathode, (3) Ni-cermet anode, (4) current collector of Pt wire, (5) metallic construction, (6) metallic spring, (7) metallic rod, (8) porous ceramic insertions, (9) thermocouple, (10) copper current collectors, and (11) furnace.

standard ceramic technology and the cellulose precursor technique [21]. The experimental techniques of the standard ceramic synthesis, fabricating and testing manganite cathode layers were reported in detail elsewhere [10,12–15]. The data on crystal structure, thermal expansion, electrical conductivity and oxygen permeability of the $La_{0.6}Sr_{0.4}MnO_{3-\delta}$ solid solution as well as the results on cathodic polarization of the LSM6 electrodes were also published earlier [10,12].

The cellulose precursor technique is based on using structure-modified cellulose containing the metal salts as a precursor for the perovskite oxide-phase synthesis. At the first stage of the synthesis, the starting cellulose fibre was reacted with a 68–70% aqueous solution of nitric acid [21,22]. The interaction of HNO_3 monohydrate with native cellulose results in the formation of an additional compound $(C_6H_{10}O_5 \cdot HNO_3)_n$ called the Knecht compound (KC), which was then converted into cellulose hydrate (cellulose-II) by the action of water. The phase transformation 'cellulose-I → KC → cellulose-II' was established to lead to increasing sorption activity of the cellulose matrix [22,23]. Incorporation of cations into the modified cellulose was then performed by impregnation with a solution containing manganese, lanthanum and strontium salts (nitrates or acetates) with the ratio between the cation concentrations set at 10:6:4 and an impregnation ratio of 1.2 ml/g. After drying in air, the cellulose fiber was ignited, and the formation of the $La_{0.6}Sr_{0.4}MnO_{3-\delta}$ oxide phase occurred in the combustion front. The oxide fibre obtained by the salt-containing cellulose combustion retains the fibre precursor texture (Fig. 3). Then the LSM6 oxide fibre with organic binder was applied onto YSZ tubes. In order to take into account the shrinkage of the electrode during its sintering, the zirconia tubes were covered with the LSM fibre two to three times, providing small wrinkles. Then the cells were slowly heated to 1470 K (heating rate of about 100 K/h) and sintered at for 2–3 h. Formation of the perovskite single phase and cation composition of the electrodes were verified by the X-ray diffraction technique (XRD), atomic emission spectroscopy (AES), and X-ray fluorescence analysis (XFA). The analysis techniques were described elsewhere [12–15,21]. One should note that the cellulose precursor technique allows to obtain oxide electrodes with highly developed surface and uniformly distributed porosity. For instance, Fig. 4 demonstrates top view of the LSM6 electrode prepared by this method.

For the anodes, we used cermets consisting of metallic nickel (76 wt.%), cerium dioxide (12 wt.%) and $Zr_{0.90}Y_{0.10}O_{1.95}$ (12 wt.%). The $Zr_{0.90}Y_{0.10}O_{1.95}$ powders were manufactured by the Eastern Research Institute of Refractories (Ekaterinburg, Russia) using a hydroxide coprecipi-

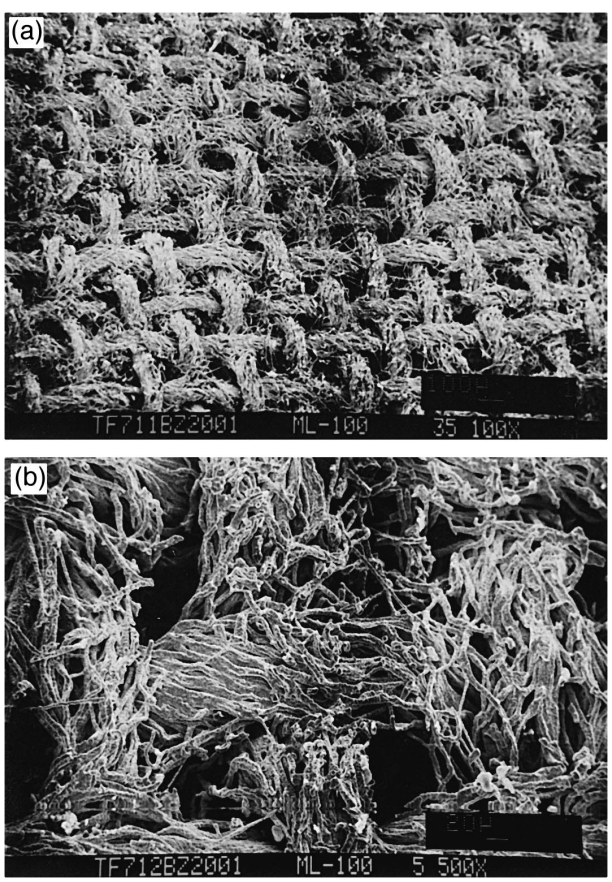

Fig. 3. (A and B) SEM micrographs of the $La_{0.6}Sr_{0.4}MnO_{3-\delta}$ oxide fibers prepared by the cellulose-precursor method after combustion of the cellulose matrix.

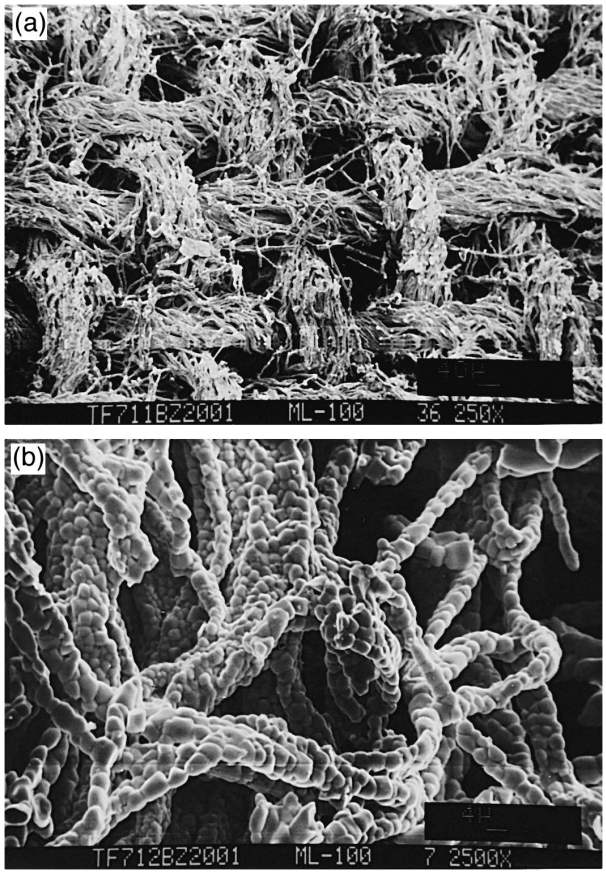

Fig. 4. (A and B) Top view of the $La_{0.6}Sr_{0.4}MnO_{3-\delta}$ electrode prepared by the cellulose-precursor method after sintering oxide fibre applied onto YSZ surface.

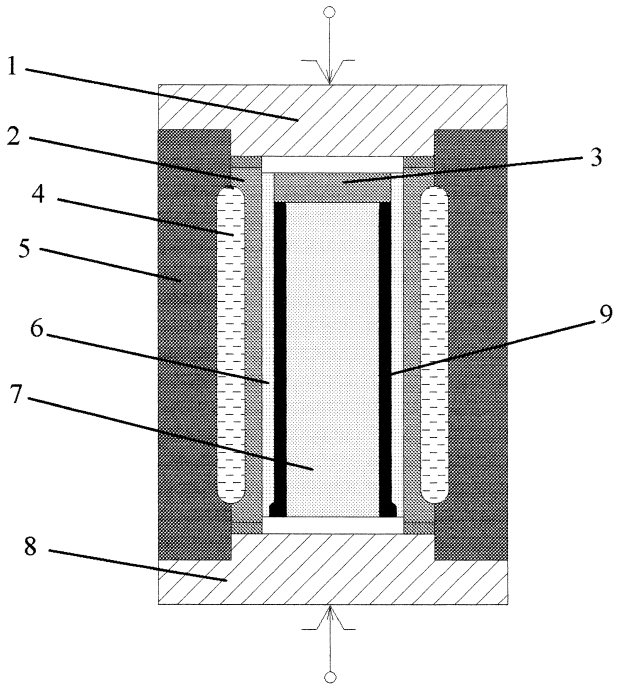

Fig. 5. Schematics of the isostatic pressing of the manganite current collectors: (1) bolt, (2) elastic insert, (3) elastic plug, (4) cavity with working liquid, (5) frame, (6) elastic envelope, (7) mandrel, (8) lower support, and (9) powder under pressing.

tation method. Cerium dioxide powder prepared by thermal decomposition of cerium nitrate was added to cermet composition on the basis of results of Refs. [5,20] showing a high electrocatalytic activity of ceria in atmospheres containing hydrocarbons and carbon oxides. The particle size of each of the cermet components did not exceed 2–3 μm. The anode layers with loading density of 25–30 mg/cm^2 were deposited onto YSZ ceramics and sintered at 1270–1320 K in a hydrogen flow.

2.3. Producing manganite current collectors

Dense tubes of $La_{0.7}Sr_{0.3}MnO_{3-\delta}$ were formed by the axial isostatic pressing technique. For this purpose, special equipment has been worked out. It enabled one to make ceramic articles having various shapes and dimensions up to 1000 mm long and 120 mm wide under pressures of no more than 300 MPa. A schematic drawing of pressing manganite tubes is shown in Fig. 5. This technology ensures even distribution of density in the volume of pressing and relatively high productivity of the pressing (15–100 ceramic articles per hour). Moreover, the virtue of the technology is its cheapness and small dimensions of the equipment. For the pressing, we used the manganite powder prepared by the standard ceramic synthesis route, similar to that described in Ref. [12]. The particle size of the manganite powder was varied from 10 to 60 μm. Plastic mixtures of the ceramic powders were obtained by first dry blending with additions of polymer (polyvinyl alcohol, 5 wt.%) and sintering aid (bismuth oxide, 4 wt.%). Then water was stirred in and the composition was milled until a uniform consistency was obtained. The tubes were pressed at 150–250 MPa and sintered at

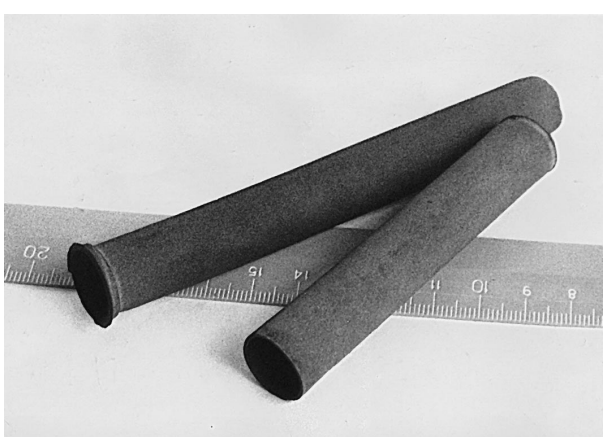

Fig. 6. Photograph of dense $La_{0.7}Sr_{0.3}MnO_{3-\delta}$ tubes used as current collectors.

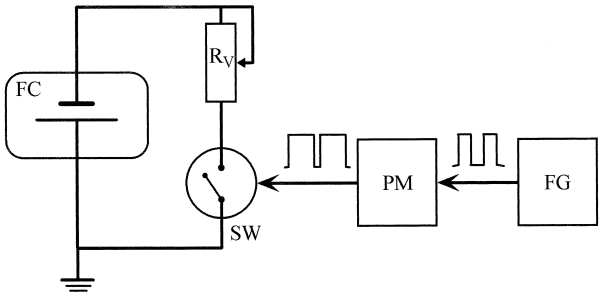

Fig. 7. Schematic setup of the measurement device for testing an SOFC with externally switched pulse load: (FC) cell under test, (R_V) variable resistor, (SW) externally driven switch, (FG) frequency generator, and (PM) pulse period-to-pulse duration ratio modulator.

1770–1820 K for 15 h in atmospheric air. A photograph of the dense LSM7 tubes is presented in Fig. 6.

2.4. Testing cells

For the performance tests of the SOFCs, atmospheric air was used as the oxidant gas and converted propane as the fuel. Temperature of the tests was varied in the range of 1040–1270 K. Propane gas was converted into a mixture of carbon oxides, hydrogen and water vapor by the reaction with atmospheric air. The conversion was performed in a standard reactor at temperatures of 820–970 K on Pt/Al_2O_3 catalysts produced by the Institute of Catalysis (Novosibirsk, Russia). The reactor was connected consequently to the SOFC under tests, supplying a required fuel gas mixture to anode. The ratio between air and propane fluxes fed into the conversion reactor was chosen to vary open-circuit voltage (OCV) of the SOFC in the range from 0.78 to 1.2 V. In the course of each experiment, the OCV values were maintained to be constant with an accuracy of ± 10 mV. The time of a steady-state attainment for the tested SOFCs was 10–25 h.

Fig. 7 presents schematic layout of the measurement device for testing SOFC with externally switched pulse load. The cell labeled FC was connected in series to a variable resistor *R4830 / 1* (R_V) and a switch (SW) based on a MOSFET-transistor *RFP50N05* (produced by Harris Semiconductor, 50 A $\times$ 50 V, 0.022 Ω). The switch was driven by a square-pulse voltage. The frequency of the driving signal was varied from 2 Hz to 50 kHz by a generator *G3-111* (FG), and the pulse period-to-pulse duration ratio was modulated by the device labeled as PM. For measuring voltage and current at the SOFC output, we used precision voltmeters *V7-46* (produced by BelVAR, internal resistance of 2 GΩ, measurement error less than $\pm 0.1\%$). When measuring each set of experimental values, the data were integrated and averaged for 2–3 min (6×10^3–9×10^3 of experimental points determined with a rate of 50 measurements/s). The pulse shape of the current and voltage, as well as phase difference between these quantities were studied using oscilloscopes *S7-16* and *S1-76* (BelVAR).

3. Results and discussion

Preliminary tests showed that performance of both fuel cells 1 and 2 can be significantly improved by applying catalysts onto electrode surfaces. According to the data in Refs. [5,10,20,24], cerium oxide was used to increase the electrochemical activity of anodes and praseodymium oxide for the cathodes. The surface modification technique was as follows. After assembling SOFCs and preliminary tests, cathode and anode layers were impregnated with saturated ethanol solutions of praseodymium nitrate and

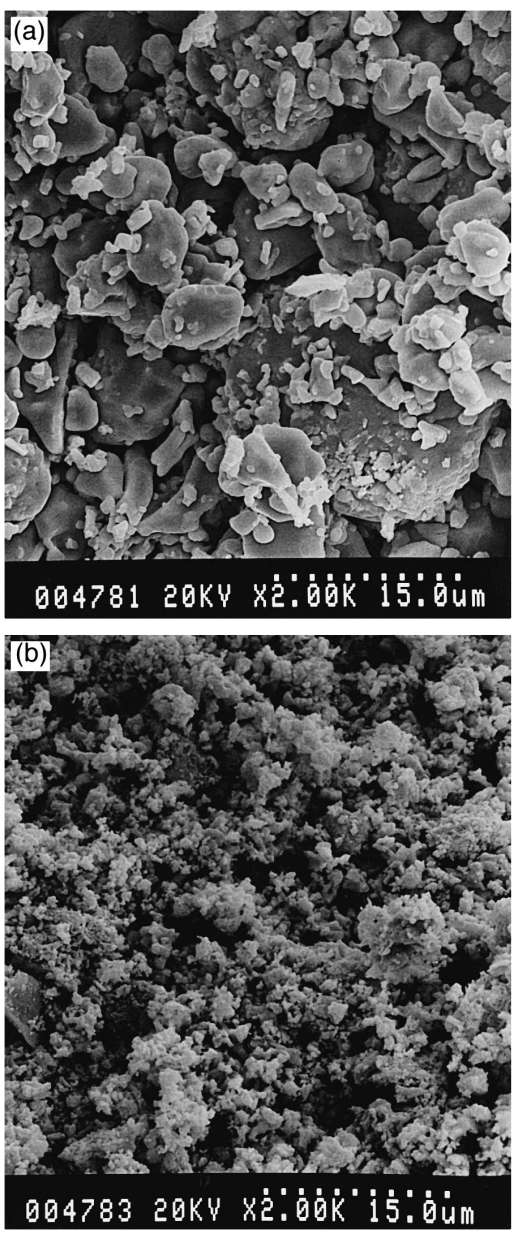

Fig. 8. SEM micrograph of LSM6 cathode prepared by the standard ceramic technique: (A) before surface modification with praseodymium oxide, and (B) after coating with dispersed praseodymium oxide.

cerium nitrate, respectively. Then the cells were slowly heated to 1270 K (heating rate of 100–150 K/h) and annealed for 2–3 h. During the annealing, fluxes of hydrogen gas and atmospheric air were supplied into anode and cathode chambers, correspondingly. As a result, highly dispersed oxide catalysts are distributed uniformly on the electrode surface, developing electrode morphology (Fig. 8). Possible mechanisms of catalytic effects of the praseodymium oxide coatings were discussed elsewhere [10]. The electrode surface modification was found to improve considerably the performance of the cells: after the activation, the power density increases by 5 to 25%. For example, Fig. 9 illustrates the effect of the electrode activation on performance of cell 2 at 1220 K. Notice that no considerable difference in performance of the cells with cathodes prepared by the solid-state synthesis and the cellulose precursor methods was observed after the electrode surface modification. Such behavior is probably associated with forming thin layers of the zirconate phases at the electrode/electrolyte interface which results in oxygen ionic current limitations. Formation of the blocking layers (topotactic reaction) was reported to occur at the interface

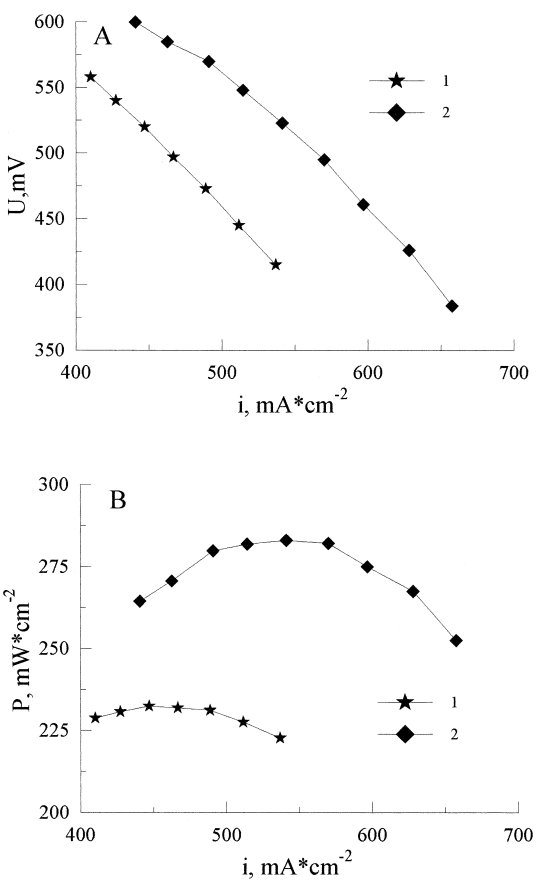

Fig. 9. Voltage vs. current density (A) and power density vs. current density (B) for cell 2 at 1220 K and OCV of 1020 mV in the steady state: (1) before surface modification, and (2) after electrode surface modification with praseodymium oxide and cerium oxide (see text).

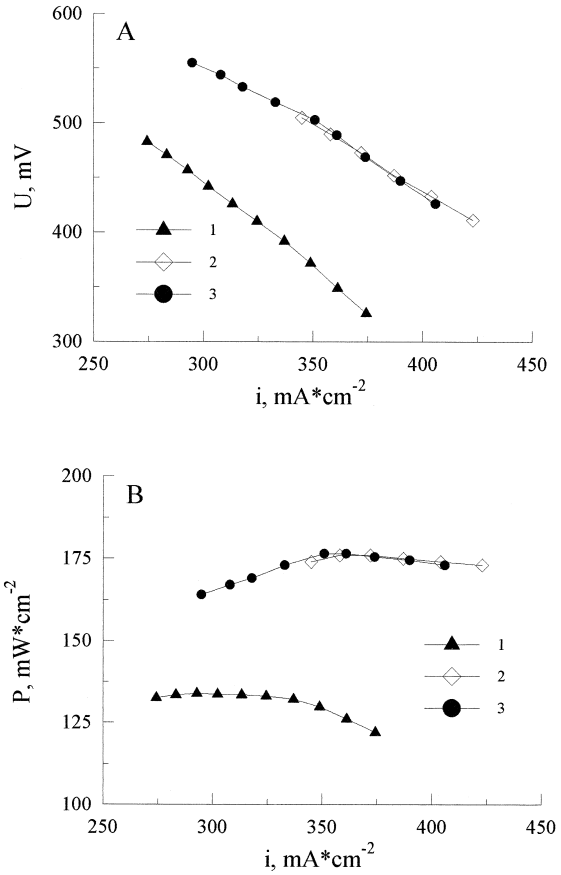

Fig. 10. Voltage vs. current density (A) and power density vs. current density (B) at 1150 K and OCV of 920 mV: (1) cell 1 in the steady state, (2) cell 2 in the steady state, and (3) cell 2 with the pulse load ($\nu = 2$ Hz, $A = 10/9$).

of the zirconia-based solid electrolyte and LSM perovskite superstoichiometric on the lanthanum sublattice [25,26]. While manganese oxide may diffuse into the YSZ ceramics from the stoichiometric lanthanum–strontium manganite, interaction between zirconia and a formed superstoichiometric perovskite phase leads to forming zirconate phases having a low ionic conductivity. Due to this, the electrode resistance increases. On the other hand, the rate-determining steps of oxygen reduction on the manganite cathodes were established to be the diffusion of O^-_{ad} species along the LSM surface and the activation process at the triple-phase boundary [27,28]. When the activity of both triple-phase boundary and electrode surface increases due to applying a catalyst, the limiting role of ionic transport through thin zirconate layers is expected to increase. Therefore, the observed negligible difference in performance of the LSM6 cathodes prepared by the different methods may be caused by the formation of the blocking layers at the interface.

The results of studying SOFCs after electrode activation in the steady-state and nonsteady-state conditions are presented in Figs. 10 and 11. At temperatures above 1120 K,

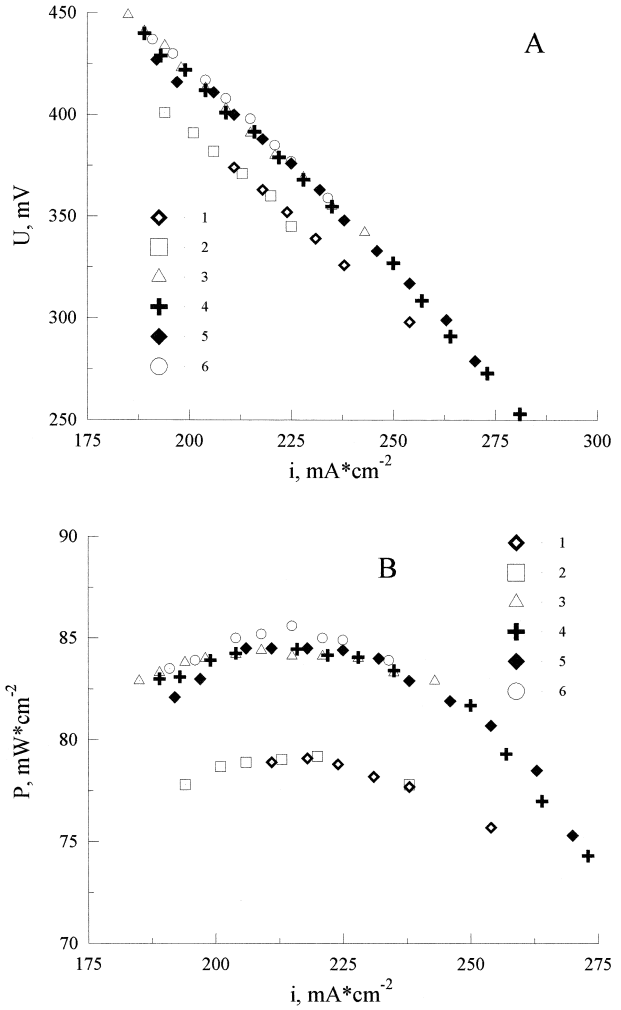

Fig. 11. Voltage vs. current density (A) and power density vs. current density (B) at 1090 K and OCV of 780 mV: (1) cell 1 in the steady state, (2) cell 1 with the pulse load ($\nu = 12$ Hz, $A = 10/8$), (3) cell 2 in the steady state, (4) cell 2 with the pulse load ($\nu = 20$ kHz, $A = 10/5$), (5) cell 2 with the pulse load ($\nu = 2$ kHz, $A = 10/9$), and (6) cell 2 with the pulse load ($\nu = 2$ Hz, $A = 10/9$).

the performance of cell 2 is substantially higher in comparison with that of cell 1, which is caused by the LSM tube current collector resistance. Decreasing temperature results in an increasing role of polarization losses and resistance of the solid electrolyte and electrical contacts. Correspondingly, the difference in performance of the cell 1 and 2 was observed to decrease with decreasing temperature.

The nonsteady state of the cell with externally switched pulse load is characterized by the quantities of the frequency (ν) and the pulse period-to-pulse duration ratio (A), expressed by the formula:

$$A = (\tau/\tau_1) = (\nu\tau_1)^{-1}, \quad (1)$$

where τ and τ_1 are the period and durability of the pulses closing the circuit with a resistor, respectively. The quantity $(A-1)/A$ refers to the fraction of time when the circuit is open. Respectively, the quantity

$$1 - \frac{A-1}{A} = A^{-1} \quad (2)$$

represents the fraction of time when the circuit is closed. The effective resistance of the external circuit ($\bar{R}$) is determined by the equation

$$\bar{R} = \left[\frac{1}{R_1 A} + \frac{1}{R_2}\left(1 - \frac{1}{A}\right)\right]^{-1} = \frac{R_1 R_2 A}{R_2 + R_1(A-1)}, \quad (3)$$

where R_1 and R_2 are the values of the resistance of the circuit with closed switch and the circuit with open switch, respectively. In the studied case, $R_2 \to \infty$ and

$$\bar{R} = \left[\frac{1}{R_1 A} + \frac{1}{R_2}\left(1 - \frac{1}{A}\right)\right]^{-1} \approx AR_1. \quad (4)$$

Testing SOFCs under nonstationary conditions demonstrated that the externally switched pulse load can be effectively applied to optimize the SOFC operating regime without reducing performance. In the studied range of frequency (2 Hz–50 kHz) and the pulse period-to-pulse duration ratio (from 10/9 to 10/4), the difference between power density of the cells in different conditions was ascertained to be within experimental error limits. No effect of the frequency on the SOFC performance was found. The most probable reason for the observed independence of SOFC performance on the switched pulse load frequency is an absence of dissipative frequency-dependent parts of the fuel cell internal resistance in the studied range of the signal frequency spectra. Indeed, the SOFC power relaxation time after significant changes in the operation mode (such as closing circuit after prolonged open-circuit tests or a significant change of the load resistance) was observed to be of the order of some hours that corresponds to frequencies less than 10^{-4} Hz. Such relaxation times refer to the dissipative electrochemical processes (diffusion, re-distribution of oxygen vacancies in the LSM cathodes, oxidation of metallic nickel at the anode, etc.). Capacitive parts of the SOFC internal resistance, which were detected in the studied range of the signal spectra as distortions of the pulse edges observed using the oscilloscope, are assumed to be associated with the electrode double-layer capacitances. The dissipative contribution of these capacitances to the total SOFC internal resistance is negligible.

Thus, one can provide optimum SOFC operation mode at a given resistance of the closing external load by selecting A values. The results obtained demonstrate an applicability of the externally switched pulse load to match resistances of single cells in the SOFC stacks.

4. Conclusions

Experimental methods of fabricating tubular-type SOFC with cathodes and current collectors of lanthanum–

strontium manganite are described. Particular emphasis is given to the techniques of preparing oxide electrodes via cellulose precursor decomposition, isostatic pressing of the manganite tubes, as well as surface activation of SOFC electrodes. Applying dispersed ceria onto anode surface and praseodymium oxide onto cathode surface was established to increase considerably SOFC performance. The maximum power density of the tested cells was about 280 $mW \times cm^{-2}$ at 1220 K. It was demonstrated that matching resistances of single fuel cells in the SOFC stack can be achieved by variation of the pulse period-to-pulse duration ratio of the externally switched pulse load connected to each cell. Therewith, no effect of the pulse load frequency on cell performance was observed in the studied frequency range (2 Hz–50 kHz).

Acknowledgements

This work was partially supported by the Belarus Ministry of Education and Science, the Belarus Foundation for Fundamental Research and by the Belarus Soros Foundation.

References

[1] M.C. Williams, in: M. Dokiya, O. Yamamoto, H. Tagawa, S.C. Singhal (Eds.), Solid Oxide Fuel Cells IV, Vol.95-1, The Electrochemical Society, Pennington, USA, 1995, p. 10.
[2] P. Stonehart, in: U. Bossel (Ed.), Proc. 1st European SOFC Forum, Vol. 1, Lucerne, Switzerland, 1994, p. 15.
[3] N.Q. Minh, J. Am. Ceram. Soc. 76 (1993) 563.
[4] K. Kinoshita, Electrochemical Oxygen Technology, Wiley-Interscience, New York, 1992.
[5] B.C.H. Steele, in: U. Bossel (Ed.), Proc. 1st European SOFC Forum, Vol. 1, Lucerne, Switzerland, 1994, pp. 375–397.
[6] S.C. Singhal, in: F.W. Poulsen, N. Bananos, S. Linderoth, M. Mogensen, B. Zachau-Christiansen (Eds.), Proc. 17th Riso Int. Symp. on Materials Science, Roskilde, Denmark, 1996, p. 123.
[7] C.W. Tanner, K.-Z. Fung, A.V. Virkar, J. Electrochem. Soc. 144 (1997) 21.
[8] K. Ravindranathan Thampi, A.J. McEvoy, J. Van herle, J. Electrochem. Soc. 142 (1995) 506.
[9] M. Watanabe, H. Uchida, M. Shibata, N. Mochizuki, K. Amikara, J. Electrochem. Soc. 141 (1994) 342.
[10] V.N. Tikhonovich, V.V. Kharton, E.N. Naumovich, A.A. Savitsky, Solid State Ionics 106 (1998) 197.
[11] K. Sasaki, J.P. Wurth, M. Goedickemeier, A. Mitterdorfer, L.J. Gauckler, in: U. Bossel (Ed.), Proc. 1st European SOFC Forum, Vol. 1, Lucerne, Switzerland, 1994, p. 475.
[12] V.V. Kharton, A.V. Nikolaev, E.N. Naumovich, A.A. Vecher, Solid State Ionics 81 (1995) 201.
[13] V.V. Kharton, E.N. Naumovich, A.A. Vecher, A.V. Nikolaev, in: O. Savadogo, P. Roberge, T. Veziroglu (Eds.), Proc. 1st Int. Symp. on New Materials for Fuel Cell Systems, Montreal, Canada, 1995, p. 512.
[14] Yu.S. Gaiduk, V.V. Kharton, E.N. Naumovich, A.V. Nikolaev, V.V. Samokhval, Inorganic Materials 30 (1994) 1360.
[15] Yu.S. Gaiduk, V.V. Kharton, E.N. Naumovich, V.V. Samokhval, Inorganic Materials 30 (1994) 759.
[16] V.N. Tikhonovich, V.V. Kharton, E.N. Naumovich, Inorganic Materials 33 (1997) 602.
[17] S. Carter, A. Selcuk, R.J. Chater, J. Kajda, J.A. Kilner, B.C.H. Steele, Solid State Ionics 53–56 (1992) 597.
[18] B.A. van Hassel, T. Kawada, N. Sakai, H. Yokokawa, M. Dokiya, H.J.M. Bouwmeester, Solid State Ionics 66 (1993) 295.
[19] A.V. Kovalevsky, V.V. Kharton, V.N. Tikhonovich, E.N. Naumovich, A.A. Tonoyan, O.P. Reut, L.S. Boginsky, Mat. Sci. Eng. B 52 (1998) 105.
[20] M.V. Perfilyev, A.K. Demin, B.L. Kuzin, A.S. Lipilin, High-Temperature Electrolysis of Gases, Nauka, Moscow, 1988, in Russian.
[21] V.V. Kharton, V.N. Tikhonovich, Li Shuangbao, E.N. Naumovich, A.V. Kovalevsky, A.P. Viskup, I.A. Bashmakov, A.A. Yaremchenko, J. Electrochem. Soc. 145 (1998) 1363.
[22] L.V. Solovéva, I.M. Grigoréva, T.F. Tikhonova, I.A. Bashmakov, F.N. Kaputskii, Vestsi AN Belarusi (Letters of Belarus Academy of Sciences), ser. chem. 3 (1994) 57, in Russian.
[23] E.V. Gert, Cellulose 3 (1996) 217.
[24] G.I. Fadeev, M.V. Perfilyev, in: M.V. Perfilyev (Ed.), Electrode Processes in Solid-Electrolyte Systems, Ural Department of the Academy of Science of USSR, Sverdlovsk, Russia, 1988, pp. 85–95, in Russian.
[25] E. Syskakis, G. Stochniol, A. Naoumides, H. Nickel, Proc. 2nd Int. Conf. on Ceramics in Energy Applications, London, 1994, p. 91.
[26] T. Tsai, S.A. Barnett, Solid State Ionics 93 (1997) 207.
[27] H.Y. Lee, W.S. Cho, S.M. Oh, H.-D. Wiemhoefer, W. Gopel, J. Electrochem. Soc. 142 (1995) 2659.
[28] F.H. van Heuveln, H.J.M. Bouwmeester, J. Electrochem. Soc. 144 (1997) 134.